Low frequency finite element models of the acoustical behavior of earmuffs

Sylvain Boyer and Olivier Doutres
Department of Mechanical Engineering, École de technologie supérieure, 1100 rue Notre-Dame Ouest, Montréal, Québec H3C 1K3, Canada

Franck Sgard[a)]
IRSST, Direction Scientifique, 505 Boulevard de Maisonneuve Ouest, Montréal, Québec H3A 3C2, Canada

Frédéric Laville
Department of Mechanical Engineering, École de technologie supérieure, 1100 rue Notre-Dame Ouest, Montréal, Québec H3C 1K3, Canada

Jérôme Boutin
IRSST, Service de la recherche, 505 Boulevard de Maisonneuve Ouest, Montréal, Québec H3A 3C2, Canada

(Received 4 May 2014; revised 11 December 2014; accepted 8 April 2015)

This paper compares different approaches to model the vibroacoustic behavior of earmuffs at low frequency and investigates their accuracy by comparison with objective insertion loss measurements recently carried out by Boyer *et al*. [(2014). Appl. Acoust. **83**, 76–85]. Two models based on the finite element (FE) method where the cushion is either modeled as a spring foundation (SF) or as an equivalent solid (ES), and the well-known lumped parameters model (LPM) are investigated. Modeling results show that: (i) all modeling strategies are in good agreement with measurements, providing that the characterization of the cushion equivalent mechanical properties are performed with great care and as close as possible to *in situ* loading, boundary, and environmental conditions and that the frequency dependence of the mechanical properties is taken into account, (ii) the LPM is the most simple modeling strategy, but the air volume enclosed by the earmuff must be correctly estimated, which is not as straightforward as it may seem, (iii) similar results are obtained with the SF and the ES FE-models of the cushion, but the SF should be preferred to predict the earmuff acoustic response at low frequency since it requires less parameters and a less complex characterization procedure. © *2015 Acoustical Society of America*. [http://dx.doi.org/10.1121/1.4919326]

[KML] Pages: 2602–2613

I. INTRODUCTION

A widespread solution used to protect the worker from noise exposure consists in using hearing protection devices (HPDs), such as passive earmuffs. Earmuffs are typically made up of a plastic cup filled with a foam insert and a comfort cushion attached to the cup through a back plate (see Fig. 1). The cushion ensures an acoustic sealing between the skin and the cup, and guarantees a certain comfort to the user.

The use of passive earmuffs is, however, associated with three main issues. First, they can affect the acoustical and physical comfort of the worker thereby inducing a reduction of the earmuff wearing time and an increase in his noise exposure (Gerges, 2012). Second, there remain issues associated with measurement methods to assess the real protection brought by earmuffs in the workplace, such as the field measurement in real ear. In particular, the effect of the position of the outer and inner microphones on the earmuff noise attenuation (NR) has not been studied yet and the compensation factors to be used to relate NR and the insertion loss (IL) are still unknown. Third, there is a lack of tools to optimize the acoustical design of the earmuffs. Various analytical and numerical models have been proposed in the past to predict the vibroacoustic behavior of earmuffs. They are briefly reviewed next.

The analytical models are usually lumped parameters models (LPMs), such as the one developed by Zwislocki (1955), Shaw and Thiessen (1958), Paurobally and Pan (2000), Sides (2004), Du and Homma (2009), and Kalb (2010). They are used to model the sound attenuation of circumaural HPDs at low frequency, typically <1 kHz. They consider the plastic cup as a rigid mass attached to a spring-damper system representing the cushion in parallel with the air cavity stiffness enclosed by the earmuff. This system exhibits a mass-spring resonant response called pumping motion, which occurs typically between 100 Hz and 300 Hz. This modeling strategy is useful to approximate the behavior of the earmuff, but it is limited to low frequencies, i.e., below the first acoustic or elastic structural resonance of the system. To overcome this limitation, numerical models based on the finite element method (FEM) or the boundary element method (BEM) have been proposed (Lee *et al*., 1995; Vergara *et al*., 2002; Anwar, 2005; James, 2006; Khani *et al*., 2007; Du and Homma, 2009; Sgard *et al*., 2010). They are able to predict the vibroacoustic behavior of earmuffs over a large frequency band, typically up to 5 kHz.

a)Electronic mail: franck.sgard@irsst.qc.ca

 0001-4966/2015/137(5)/2602/12/$30.00

Furthermore, the solid and fluid domains are modeled geometrically, and couplings are naturally accounted for through continuity conditions of displacements and stress vectors. The FEM or BEM modeling strategies are promising predicting tools to capture the trends of the earmuff vibroacoustic behavior. However, the choice of the various FEM-BEM models proposed for the different HPD components have never been clearly justified and have not been compared to each other. This is especially true for the cushion, which is either modeled using equivalent spring elements or as an equivalent linear isotropic elastic material.

As underlined by Shaw and Thiessen (1958), the sound attenuation of earmuffs at low frequencies (i.e., around the pumping motion resonance) is mainly controlled by the combined stiffness of the cushion and the air cavity, and by the mass of the cup. The cushion component is, undoubtedly, the trickiest component to characterize for both FEM and LPM modeling strategies because of its physical complexity. The cushion is generally made of a foam piece surrounded by a polymeric sheath, which ensures the seal between the skin and the plastic cup. Vent holes are made either through the sheath or sometimes through the back plate to allow for the cushion to deflate when subjected to the headband force. This multi-domain component presents, therefore, a real modeling challenge as the cushion model must be able to capture both the suspension mechanical effect at low frequencies and the sound transmission through its lateral walls at mid frequencies (Boyer *et al.*, 2014) and possibly the effect of the vent holes. An additional difficulty lies in the fact that the cushions are made from polymer materials whose mechanical properties depend on frequency, temperature, and dynamic and static compression rate; the latter parameter being set by the headband force (Boyer *et al.*, 2011). Because of all these issues, the cushion stiffness used in the LPM models is usually assessed from curve fitting of IL experimental data and is considered frequency independent.

The goal of this paper is to compare the LPM and FEM modeling strategies at low frequencies (i.e., $f < 500$ Hz). In the case of the FEM, the cushion is either modeled as a spring foundation (SF) or as an equivalent isotropic viscoelastic solid (ES). In the SF model, the cushion only deforms along its thickness and no sound can be transmitted through its lateral walls. This model does not require meshing the cushion volume, which thus reduces significantly the computation time. On the contrary, the ES model allows for cushion tridimensional elastic deformations and a possible sound transmission through its lateral walls. Two commercial earmuffs with different designs are investigated (their respective components are presented in Fig. 1): the EAR-MODEL1000 (3M^{TM} E-A-R^{TM}, Indianapolis, USA) already studied in Lee *et al.* (1995), Vergara *et al.* (2002), Khani *et al.* (2007), Sgard *et al.* (2010), Boyer *et al.* (2011), Boyer *et al.* (2013), Berger *et al.* (2012), and the PELTOR-OPTIME-98 (3M^{TM} Peltor^{TM}, Indianapolis, USA) (to the authors' knowledge, no acoustical model was developed previously for this earmuff). The two earmuff models mainly differ by their respective cushion design. The EAR-MODEL-1000 cushion is made of a flexible foam surrounded by a polymeric sheath; the whole being glued to the back plate by the use of an adhesive plastic tape included to the bottom face of the sheath. The PELTOR-OPTIME-98 has a built-in back plate cushion, which is clipped to the ear cup. This foam-filled cushion contains a gel pouch thermoformed with the back plate and the sheath. In the following, the earmuffs are considered to lie on a rigid baffle [see Figs. 1(c) and 1(d)], with a perfect sealing between the cushion and the baffle.

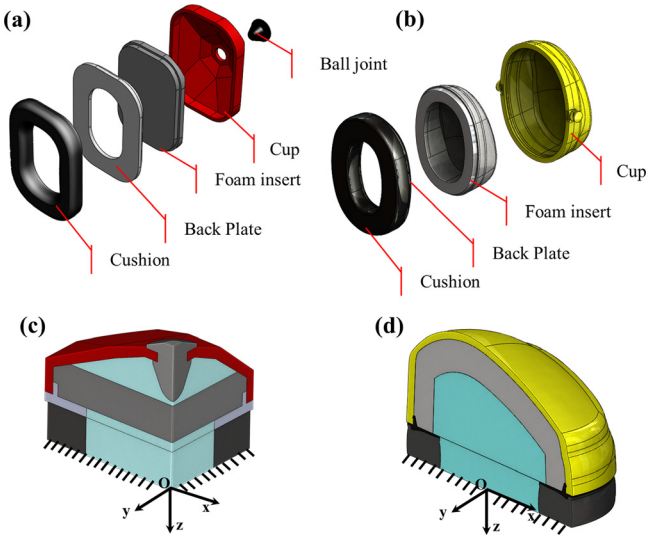

FIG. 1. (Color online) Components of the (a) EAR-MODEL-1000 earmuff and (b) PELTOR-OPTIME-98; CAD geometries of the (c) EAR-MODEL-1000 and (d) PELTOR-OPTIME-98. The earmuff is located in the negative z-space and lies on the baffle at $z = 0$.

A thorough characterization of the two types of foam-filled cushions equivalent mechanical parameters as a function of frequency and static compression is performed at very low frequencies ($f < 60$ Hz) using two experimental setups and a rheological model of viscoelastic materials. Due to the viscoelastic nature of the cushion components, much effort is made to carry out the characterization procedure using loading, boundary, and environmental conditions as close as possible from the ones set during the acoustic tests. Whereas the equivalent complex stiffness required in both the LPM and SF modeling strategies is directly assessed from the characterization experimental setups, the equivalent Young's modulus required in the ES approach is estimated by an inverse hybrid method combining measurements and a structural FEM model of the characterization experimental setup. The equivalent mechanical properties (i.e., stiffness or Young's modulus and loss factor) are then extrapolated at higher frequency using a four-parameter fractional derivative Zener (FDZ) model. The necessity to account for their frequency dependence in order to predict accurately the earmuff attenuation at the pumping resonance is underlined. The attenuations calculated using the two FEM models are compared to each other and to experimental data presented in Boyer *et al.* (2014). Finally, this work examines the accuracy of a LPM by comparing different empirical formulations to approximate the earmuff internal air cavity stiffness to the experimental results.

The paper is organized as follows. Section II presents the various LPM formulations used in the literature. Section

III describes the earmuffs FE models together with the two modeling strategies (SF and ES) for the cushions. The characterization procedure to determine the equivalent mechanical properties of the cushions is detailed in Sec. IV. Finally, Sec. V compiles and discusses the comparisons between the model predictions and the acoustical measurements.

II. LPMs FORMULATIONS

LPMs are the easiest ways to predict the low frequency response of earmuffs. In the case of a perfect sealing between the cushion and the baffle and the foam insert being removed from the cup, the sound attenuation of the earmuff given by the analytical models (Zwislocki, 1955; Shaw and Thiessen, 1958; Paurobally and Pan, 2000; Sides, 2004; Du and Homma, 2009) can be expressed as

$$\mathrm{Att} = p_i/p_o = A(k_{\mathrm{air}}/(-\omega^2 m + (k_{\mathrm{air}} + k) + j\omega c)), \quad (1)$$

where p_i and p_o are the sound pressures applied, respectively, on the inner (S_i) and outer (S_o) boundaries of the earmuff, j is the imaginary unit ($j^2 = -1$), m represents the mass of the cup, k is the equivalent stiffness of the cushion, and c is the cushion viscous damping coefficient, which can be expressed as a function of the structural loss factor of the cushion, $\eta : c = \eta\sqrt{mk}$. $k_{\mathrm{air}} = \rho c^2 S_r^2/V_r$ is the air cavity stiffness assumed to be similar to that of a cylindrical volume, V_r, of circular cross section, S_r, enclosed by the earmuff, ρ and c are the air cavity density and sound speed, respectively. A is a term accounting for the thickness of the plastic cup. For Sides (2004), $A = S_o/S_i$, while for Du and Homma (2009) and other authors, $A = 1$ and, thus, $S_o = S_i$.

It should be noted that the definitions of S_o, S_i, and S_r remain ambiguous. S_o and S_i are the areas on which the outer and inner sound pressures, respectively, act, but they are commonly assumed to be equal to the areas projected onto the baffle. In addition, two formulations of S_r can be found in the literature. In the first one, S_r is defined as the area "covered by the earmuff" (Zwislocki, 1955; Shaw and Thiessen, 1958; Paurobally and Pan, 2000; Du and Homma, 2009); see Fig. 2(a). This formulation is referred to as the Du and Homma formulation in the rest of the paper. The drawings provided in these publications depict the earmuff as a hemispherical cross section and S_r is evaluated using the cup mid surface. Consequently, the lateral cushion's thickness is not accounted for and, thus, S_r is equal to the projected area, S_o. A second expression is given by Sides (2004): $S_r = \sqrt{S_i S_S}$, where S_S and S_i are the area of the air cavity surrounded by the cushion projected onto the baffle and the earmuff inner boundary area projected onto the baffle, respectively [see Fig. 2(b)]. This expression was originally suggested in Shaw (1979) and is referred to as the Sides formulation in the following. In this work, both Du and Homma's and Sides's formulations are applied to predict the sound attenuation of the two studied commercial earmuffs. For comparison purposes and in order to remove any ambiguity, the Sides formulation is also computed considering the developed areas for S_o and S_i instead of the projected areas. Indeed, the use of developed areas seems *a priori* more consistent with the definition of S_o and S_i.

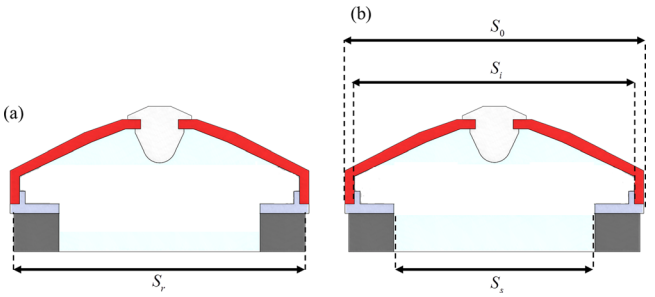

FIG. 2. (Color online) Area terms used in the analytical LPM models: (a) definitions found in Shaw and Thiessen (1958, 1962), Shaw (1979), Paurobally and Pan (2000), and Du and Homma (2009), (b) definition used by Sides (2004).

The cup mass is directly assessed using a scale, while the volume enclosed by the earmuff and the different projected or developed areas are precisely estimated from the Computer Aided Design (CAD) software. The equivalent mechanical properties of the cushion, i.e., its stiffness and its loss factor, are measured according to the procedure described in Sec. IV. All input parameters required in the LPM (except for the cushion stiffness, k, and loss factor, η) are given in Table I.

TABLE I. Input parameters for the LMP models of the EAR-MODEL-1000 and the PELTOR-OPTIME-98.

	Parameters	EAR-MODEL-1000	PELTOR-OPTIME-98
	Cup mass (back plate included) (g)	68	81.2
	V_r Air cavity volume (mm^3)	130 306	206 679
	S_S (mm^2)	2342	2123
	$S_r^{(1)}$ (mm^2) (Du and Homma, 2009)	6701	7144
Projected area onto the baffle	S_o (mm^2)	7089	7293
	S_i (mm^2)	6137	6020
	$A = S_o/S_i$	1.155	1.211
	$S_r^{(2)} = \sqrt{S_i \cdot S_S}$ (mm^2) (Sides, 2004)	3791	3575
Developed area	S_o^{dev} (mm^2)	12 321.38	15 261
	S_i^{dev} (mm^2)	13 923.63	16 012.02
	$A^{\mathrm{dev}} = S_o^{\mathrm{dev}}/S_i^{\mathrm{dev}}$	0.885	0.953
	$S_r^{(2,\mathrm{dev})} = \sqrt{S_i \cdot S_S}$ (mm^2) (Sides, 2004)	5710.88	5830.72

III. FEM MODEL OF EARMUFFS

A. General considerations

The numerical model of the baffled earmuff is implemented in the commercial FEM software COMSOL Multiphysics (COMSOL®, Stockholm, Sweden). The geometry and the orientation of the model are illustrated in Fig. 1. The bottom face of the cushion is located in the plane $z = 0$, and the earmuff lies in the negative z-space. The FEM models were simplified by using symmetry planes in order to decrease the total number of degrees of freedom of the final system to be solved. EAR-MODEL-1000 includes two symmetry planes: (O, x, z) and (O, y, z), while the model developed for the PELTOR-OPTIME-98 involves only one: (O, x, z).

In the following, the coupled problem is solved in the frequency domain, and all the fields are assumed to have a temporal dependency, which can be expressed as $\exp(j\omega t)$, where ω is the circular frequency. The external sound field is assumed to be an incident plane wave, which propagates in the direction normal to the baffle (direction z), and reflect onto the rigid baffle without dissipation. The sound scattering effect induced by the earmuff attached to the baffle is neglected and the sound pressure applied on the external boundaries of the earmuff (cup, back plate, and the cushion) is assumed to be $P_{\text{ext}} = P_0 \exp(-j(k_z z)) + P_0 \exp(+j(k_z z)) = 2P_0 \cos(k_z z)$, where P_0 is the amplitude and k_z are the wave number components along the z-axis. Neglecting the scattering effect is found to be a reasonable assumption for frequencies up to 500 Hz, according to more realistic simulations carried out with commercial software LMS Virtual Lab (Siemens, Munich, Germany), where the external domain is taken into account using an automatically matched absorbing layer applied on a convex acoustic volume enclosing the earmuff. These calculations are not shown here for the sake of conciseness.

Finally, the IL is chosen as the acoustical indicator to evaluate the sound attenuation. It is computed as the difference of the sound pressure level at the center of the baffle where the HPD is located, without and with the HPD

$$\text{IL} = 20\log_{10}\left(\frac{2\cdot P_0}{2e^{-5}\sqrt{2}}\right) - 20\log_{10}\left(\frac{|p(x=0,y=0,z=0)|}{2e^{-5}\sqrt{2}}\right). \quad (2)$$

B. Cup, back plate, and enclosed air cavity

The geometries of the cup and the back plate have been modeled using the CAD software SolidWorks (Dassault Systèmes®, Paris, France) based on caliper measurements for the MODEL-EAR-1000, and based on the CAD files provided by the manufacturer for the PELTOR-OPTIME-98. The cup and the back plate are modeled as linear elastic domains for both earmuffs. The corresponding material properties are given in Table II. They were measured for the earmuff EAR-MODEL-1000, while data for the PELTOR-OPTIME-98 were either measured or determined based on the datasheets provided by the manufacturer. The enclosed air cavity is modeled as a fluid domain, defined by its density ($\rho = 1.21\,\text{kg/m}^3$), and sound speed ($c = 343\,\text{m/s}$). Viscous and thermal dissipations occurring at the cavity boundaries were accounted for using a structural loss factor, $\eta_a = 1\%$, in the internal cavity.

TABLE II. Material parameters used for the earmuffs.

	EAR-MODEL-1000		PELTOR-OPTIME-98	
	Cup	Back plate	Cup	Back plate
Density (kg/m^3)	1200	1200	1040	1370
Young's modulus (GPa)	2.16	2.16	2.2	2.4
Poisson's ratio (1)	0.38	0.38	0.38	0.38
Loss factor (1)	0.05	0.05	0.05	0.05

The coupling between the structure and the internal fluid is ensured through the continuity of structural and fluid normal displacements and normal stresses at the coupling interface.

C. Cushion

1. Geometry

When the cushion is compressed by the headband force, its shape can become very complicated due to (1) bulging effects of the cushion itself and (2) the spatial inhomogeneity of the cushion static compression rate caused by a non-planar distribution of the headband force. The latter effect strongly impacts the equivalent mechanical properties of the cushion as discussed in detail in Secs. IV D and V. Despite the observed non-homogeneous cushion thickness, the geometry of the cushions is chosen as a simple annular shape whose constant thickness is equal to the minimum one (i.e., location of maximum deflection). It is considered that the modified cushion geometry due to the non-planar distribution of the headband force can be neglected. Taking into account the actual geometry of the cushion rather than a simpler one has very little effect on the earmuff IL at low frequency, as long as the equivalent mechanical parameters are correctly assessed. The geometry of each cushion has been built using the CAD software. The shape of the EAR-MODEL-1000 was an extrusion of the face that is glued to the back plate. For the PELTOR-OPTIME-98, the cushion geometry was extracted from the CAD files graciously offered by the manufacturer and was truncated to be equivalent to the compressed thickness. Note that the vents holes are not modeled here since experimental observations made by the authors showed that they did not induce a significant effect on the cushion IL.

2. SF model

The SF model is the easiest and fastest strategy to model the cushion: the cushion is modeled as a viscoelastic boundary condition applied on the back plate surface in the z-direction. The air cavity enclosed by the cushion has to be modeled as this domain participates together with the cushion to the total stiffness applied to the cup. The geometry of the cushion is therefore reproduced, but the boundary of the fluid domain, which is in contact with the cushion, is replaced by a rigid wall boundary condition. Thus, the sound transmission through the lateral walls of the cushion is not

taken into account in this model. This is a reasonable assumption since, at low frequency, the acoustical behavior of the cushion is governed by the resonance of the pumping motion rather than the sound transmission through its flanks (Boyer *et al*., 2014).

The SF model requires the knowledge of an equivalent stiffness, k, and an equivalent loss factor, η, which are determined from the characterization procedure detailed in Sec. IV. Furthermore, a distributed mass equal to one third of the mass of the sheath and the foam garniture is added on the back plate boundary connected to the cushion in order to account for the cushion mass (Rodriguez and Gesnouin, 2007). In the case of the PELTOR-OPTIME-98, the mass of the oil pouch (13.6 g) represents 76% of the total mass of the cushion (17.8 g) without the back plate (10 g). This oil pouch is modeled as a distributed mass on the back plate boundary to which the oil pouch is connected.

3. ES model

In order to allow for cushion three-dimensional (3D) elastic deformations, the earmuff cushion is modeled as a homogeneous isotropic linear viscoelastic solid. The use of a solid domain increases the realism and should allow one to better account for the coupling between the cushion and the back plate at higher frequencies (this will be investigated in a forthcoming paper). It also allows for possible flanking sound paths, which are not negligible at higher frequencies (Boyer *et al*., 2014). The physical and mechanical properties of this equivalent material are: the density, ρ, the Young's modulus, E, the loss factor, η, and the Poisson's ratio, ν. The equivalent density, ρ, of each cushion is determined using a scale with an accuracy of 0.01 g, and the CAD software is used to estimate the compressed cushion volume of the deformed simplified geometry. The fluid pouch of the PELTOR-OPTIME-98 cushion was again modeled as an added mass attached to the back plate. The loss factor, η, of the ES model is taken equal to that of the SF model and is assessed directly following the procedure detailed in Sec. IV A. Finally, the two remaining mechanical properties (E,ν) are determined using an inverse approach based on equivalent stiffness measurements and a FEM structural model of the measurement setup (see Sec. IV B).

IV. CUSHION EQUIVALENT MECHANICAL PROPERTIES

The cushion is made of a complex assembly of viscoelastic materials whose equivalent mechanical parameters depend on temperature, time of compression, static and dynamic compression rates, and frequency. The equivalent mechanical properties should, therefore, be characterized using loading, boundary, and environmental conditions as close as possible to those set during the acoustic tests. This section describes a characterization procedure of the cushion equivalent mechanical parameters required in the models based on two experimental setups and a rheological model of viscoelastic materials. The focus is put on the effect of the static compression rate and the frequency dependence of the equivalent mechanical parameters. The effect of temperature on the cushion equivalent mechanical parameters is not investigated in this work since both the characterization procedure and the acoustic measurements were carried out at a similar room temperature $\sim$22 °C.

A. Experimental setups to measure the equivalent complex stiffness

The resonant characterization method described by Sgard *et al*. (2010) and Boyer *et al*. (2011) and shown in Fig. 3(a) is used to estimate the cushion equivalent complex stiffness from low to high compression rates. The cushion is mounted on a shaker and submitted to the weight of a mass calibrated to reproduce the desired compression rate. The vibration transmissibility is measured using two accelerometers mounted on the excitation plate and the mass. The cushion equivalent stiffness and equivalent loss factor are determined at the resonance frequency of the system, typically between 25 Hz and 40 Hz, by curve fitting a simple spring/dashpot/mass model.

A quasistatic measurement analysis (QMA) method is also used to assess the frequency dependence of the complex equivalent stiffness. This method was originally used to characterize the mechanical properties (E,η,ν) of viscoelastic homogeneous or heterogeneous material specimen with cylindrical shapes. The description of the experimental setup can be found in Sahraoui *et al*. (2000) and Langlois *et al*. (2001). It consists in placing the tested sample between two plates covered with sandpaper so that no sliding motion of the sample is allowed. The experimental setup used in this work can be seen in Fig. 3(b). The top plate is fixed during measurements, but is moved before measurements to statically compress the sample with an accurate tuning of the compressed thickness, while the bottom plate is used to dynamically compress the sample. It is worth noting that this characterization setup is close to realistic conditions occurring during acoustic IL tests (Boyer *et al*., 2014): the force applied by the bottom plate mimics the headband force and the top motionless plate mimics the rigid baffle. A harmonic displacement is applied to the bottom plate via a mechanical shaker. A force transducer placed on the top plate and attached to the casing measures the force transmitted through the sample. The displacement of the bottom face is obtained from an accelerometer, and the transfer function between the transmitted force and this imposed displacement (i.e., complex dynamic stiffness) is then computed. The equivalent stiffness is given by the real part of this transfer function, while the equivalent loss factor is estimated from the ratio of the imaginary part of the transfer function over its real part. The tests are performed with a 10 Hz frequency step from 10 Hz up to 60 Hz. It should be underlined that the shaker used in the QMA setup does not allow for measurements at high compression rate (i.e., $\tau_s > 10\%$), which justifies the use of the resonant method described previously.

The frequency dependent parameters for a compression rate >10% are thus determined as follows. First, a QMA measurement is carried out at low frequencies (10 Hz $< f <$ 60 Hz) for low static compression ($\tau_s \approx 10\%$) in order to get the frequency dependence of k and η in this frequency

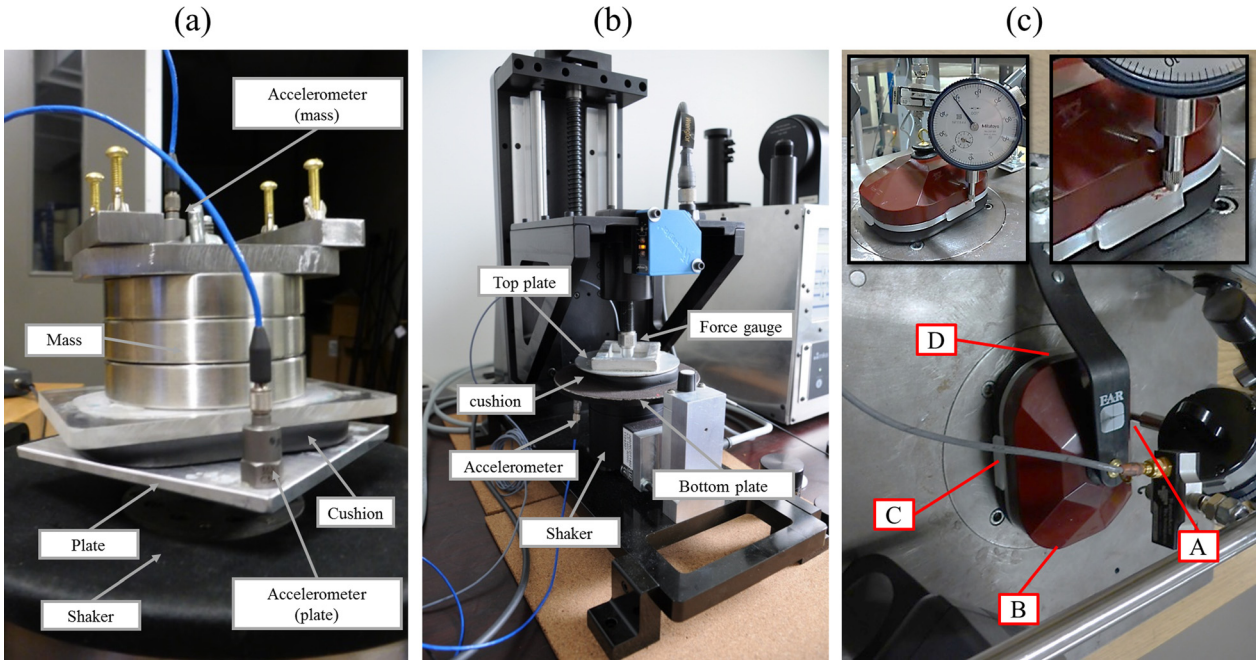

FIG. 3. (Color online) Setups used in the cushion mechanical characterization procedure: (a) resonant method, (b) quasistatic method. (c) *In situ* measurement of the cushion compression rate at four cardinal points, namely, A, B, C, and D.

range (these curves are denoted as "master curves" in the following). Second, a measurement is performed using the resonant method to assess the stiffness at the desired static compression rate ($\tau_s > 10\%$). Third, the master curves are translated along the y-axis until the point (frequency, parameter) determined using the resonance method belongs to the translated curve. An example of this procedure is given in Sec. IV D. The frequency dependence of the parameters is thus supposed to be independent from the static compression rate. This assumption relies on additional measurements carried out on a single cushion for $2.5\% < \tau_s < 10\%$ which showed that the frequency dependence does not vary significantly with the static compression rate.

B. Inverse method to estimate the equivalent Young's modulus

The equivalent complex Young's modulus required in the ES model is determined from a hybrid inverse method using the measured equivalent complex stiffness and a FEM model of the QMA experimental setup. The cushion geometry used in this FEM model is the one described in Sec. III C 1. A dynamic displacement is imposed on one side of the cushion and the reaction force along the z-direction on the opposite side of the cushion (i.e., transmitted to the rigid and motionless plate) is calculated. The Young's modulus is adjusted until the simulated equivalent stiffness matches the measured one. However, this inverse method requires the knowledge of cushion equivalent Poisson's ratio, which unfortunately cannot be measured directly for such complicated geometry. The inverse procedure was thus carried for three different values of Poisson's ratio: 0, 0.3, and 0.4. The influence of the Poisson's ratio on the computed IL is investigated in Sec. V B.

C. Compression time and dynamic compression rate

The effect of the compression time (t_e) of the cushion subjected to a constant load (i.e., headband force in the acoustic tests, mass loading in the resonant characterization method) on its equivalent stiffness was investigated, but is not presented in this paper for the sake of conciseness. A significant influence of t_e was observed during resonant tests and more particularly for $t_e < 15$ min. This effect was more pronounced in the case of the PELTOR-OPTIME-98 cushion for which a stiffness increase of 20% occurred during the first 15 min. In the following, all measurements related to characterization are carried out at $t_e = 5$ min in order to be consistent with the acoustic tests which were carried out after a compression time of 5 min (Boyer *et al.*, 2014).

The dynamic compression rate, τ_d, is expected to be very small during the IL measurements because the system is excited acoustically. All QMA measurements were thus performed with an excitation dynamic strain amplitude set to 0.04% of the sample nominal thickness. This amplitude was chosen because it ensured a linear behavior of the cushion. This parameter has not been controlled during the resonant tests, but the good agreement obtained between the two characterization methods for a given static compression rate (see Sec. IV D) indicates that the cushion behaved linearly during the resonant method.

D. Static compression rate

The cushion static compression rate, τ_s, imposed by the headband force has already been identified as one of the most important parameters affecting the cushion mechanical behavior (Anwar, 2005; Boyer *et al.*, 2011). This parameter is therefore measured *in situ* on the experimental test rig used during the IL measurements (Boyer *et al.*, 2014) as

TABLE III. Static compression rate measured *in situ* at four locations on the cushion [see Fig. 3(c)].

	A	B	C	D
EAR-MODEL-1000	13.6	19.3	10.2	9.3
PELTOR-OPTIME-98	23.2	31.1	22.6	10.8

shown in Fig. 3(c). The cushion deflection is assessed at four different locations around the earmuff using a plastic blade glued on the cup. The cushion nominal thickness (i.e., thickness of the uncompressed cushion) is measured using a caliper at the same locations. The compression rate is found to vary between 9.3% and 19.3% for the EAR-MODEL-1000 and between 10.8% and 31.1% for the PELTOR-OPTIME-98. τ_s results for all locations are given in Table III. It is shown that the test rig used to apply the headband force during the acoustical tests results on a large spatial inhomogeneity as far as τ_s is concerned. For both HPDs, the maximum (respectively, minimum) compression occurs at position B (respectively, position D) of the earmuff.

Resonant and quasistatic measurements are then carried out using the *in situ* measured static compression rates. These measurements are then coupled in order to get the frequency dependent curves (at low frequency) as explained previously. The results are presented in Figs. 4(a), 4(b), 4(d), and 4(e). For both HPDs, quasistatic measurements are performed at $\tau_s = 10\%$ (see thick gray dashed line) and resonant measurements are carried out at a static compression rate as close as possible to the ones measured *in situ* (see plain square, plain triangle, and plain circle). First, it is shown that the two characterization methods provide identical results when τ_s is set to the same value of 10%. Second, as expected, the equivalent stiffness assessed with the resonant method increases when the compression rate increases. This is coherent with what has been reported in Shaw and Thiessen (1962) and Paakkonen (1992); that is, as the headband force increases, the equivalent cushion stiffness increases and, thus, the attenuation at low frequencies also increases. However, this trend is much less pronounced in the case of the PELTOR-OPTIME-98, most probably because the sheath rigidity of its cushion is much lower compared to that of the EAR-MODEL-1000. Two different tendencies are observed for the loss factor, depending on the HPD model. In the case of the EAR-MODEL-1000, the loss factor is slightly affected by the cushion's compression rate and the frequency [Fig. 4(b)], while for the PELTOR-OPTIME-98, it increases significantly with both the compression rate and the frequency [Fig. 4(e)] and reaches unexpected high values for $\tau_s > 20\%$. This difference of behavior between the two HPDs may come from the oil pouch constituting the PELTOR-OPTIME-98 cushion. However, it is also suspected that this very important value [i.e, see plain circle in Fig. 4(e)] can be attributed to a damping added by the resonant characterization setup.

The frequency-dependent measured equivalent stiffness and loss factor obtained from the two characterization setups described previously (see Sec. IV A) are presented with x-marks for both HPDs in Figs. 4(a), 4(b), 4(d), and 4(e). These curves are only calculated at $\tau_s = 19.8\%$ for the EAR-MODEL-1000 and at $\tau_s = 33.5\%$ for the PELTOR-OPTIME-98. This choice will be explained later. Because of

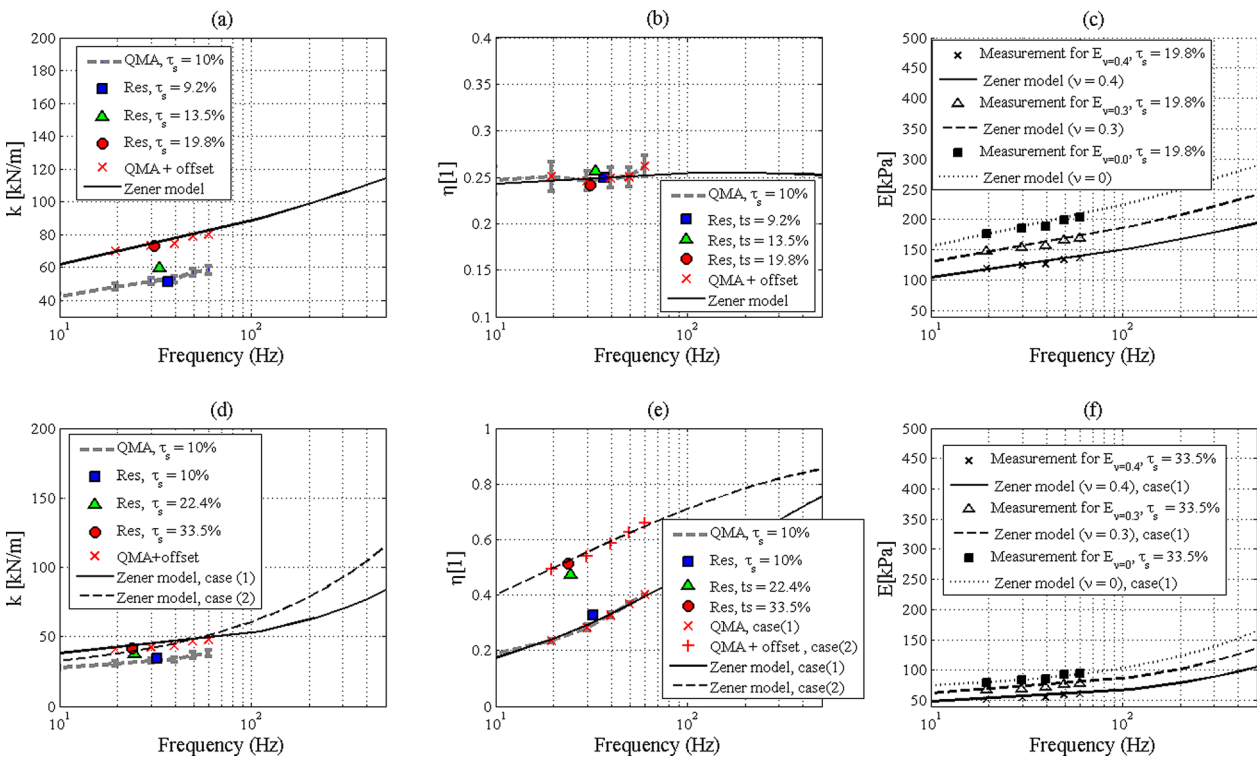

FIG. 4. (Color online) Results of the mechanical characterization of the cushions; EAR-MODEL-1000 (a) equivalent stiffness, (b) equivalent loss factor, (c) equivalent Young's modulus at a fixed Poisson's ratio; PELTOR-OPTIME-98 (d) equivalent stiffness, (e) equivalent loss factor, (f) equivalent Young's modulus at a fixed Poisson's ratio.

TABLE IV. FE models and related mechanical parameters of the EAR-MODEL-1000 cushion.

Cushion model	ρ (kg/m^3)	ν (1)	α (1)	M_0 (N/m or Pa)	M_∞ (N/m or Pa)	t_r (s)
Spring foundation	—	—	0.22555	17 044	551 023	4.91×10^{-7}
Equivalent solid	142.79	0.4	0.22297	28 127	971 750	3.74×10^{-7}
		0.3	0.21342	31 529	1 450 092	1.03×10^{-7}
		0.0	0.22034	40 798	1 518 796	2.71×10^{-7}

the very high and questionable loss factor measured for high static compression rate in the case of the PELTOR-OPTIME-98 [see Fig. 4(e)], two different frequency dependent curves of the loss factor are considered in the following; the first [denoted as case (1)] corresponds to the one obtained at $\tau_s = 10\%$ using quasistatic measurements [i.e., the master curve, see "x"-marks in Fig. 4(e)]; the second [denoted as case (2)] corresponds to the master curve, which is translated along the y-axis until it reaches the loss factor determined using the resonance method [see "+" marks in Fig. 4(e)].

Finally, the determination of the equivalent Young's modulus based on the procedure described in Sec. IV B has only been carried out at $\tau_s = 19.8\%$ for the EAR-MODEL-1000 and at $\tau_s = 33.5\%$ for the PELTOR-OPTIME-98. The inverse method has been applied for three different Poisson's ratios and the results are presented in Figs. 4(c) and 4(f). As expected, the equivalent Young's modulus decreases when Poisson's ratio increases (Langlois *et al.*, 2001).

E. Frequency dependence

The mechanical properties of viscoelastic materials are known to vary with frequency. A model of the rheological behavior of linear viscoelastic materials is thus used in this work to estimate the mechanical properties in the frequency range of interest (i.e., $80\,\text{Hz} < f < 500\,\text{Hz}$). The cushion is modeled as a viscoelastic material, which follows a fractional-derivative constitutive law: the FDZ model. The traditional FDZ model idealizes the equivalent viscoelastic material as a spring (characterized by its stiffness, M_1) and a dashpot (characterized by its viscosity coefficient, μ_1) arranged in series, which are then attached to a second spring (characterized by its stiffness, M_0) in a parallel circuit. In the FDZ model, the regular differential operators are replaced by fractional-order differential operators. This allows one to better describe the broadband frequency behavior of many viscoelastic materials with a small number of parameters (Pritz, 1996), namely, the dispersion of the dynamic modulus, the maximum loss factor, and the slope of the frequency curves. According to the FDZ model, the frequency dependent complex stiffness, M, is given by

$$M(\omega) = \frac{M_0 + M_\infty (j\omega t_r)^\alpha}{1 + (j\omega t_r)^\alpha}, \tag{3}$$

where $t_r = \mu_1 / M_1$ is the relaxation time, M_0 is the dynamic parameter at zero frequency, i.e., the static parameter, M_∞ is the high frequency limit value of the dynamic parameter (at high frequencies, the dashpot will exhibit infinite stiffness and the total stiffness of the system is simply $M_\infty = M_0 + M_1$). Finally, the loss factor is derived from $\eta(\omega) = \Im(M(\omega))/\Re(M(\omega))$, where $\Re(\cdot)$ and $\Im(\cdot)$ denote the real and imaginary part, respectively. Note that M, M_0, and M_∞ are spring stiffness coefficients expressed in N/m in the case of the LPM and SF models and are elasticity modulus expressed in Pa in the case of the ES model. The model parameters are determined by curve fitting on the low frequency measurements presented in Secs. IV A and IV B and are given in Tables IV and V. The broadband frequency dependence of the cushion mechanical parameters estimated by the four-parameter Zener model (see black lines in Fig. 4) seems realistic and consistent with the low frequency measurements. Even though this broadband estimation can be seen less valuable than a direct measurement, it is acceptable, keeping in mind the geometrical complexity of the cushion that prevents the use of more common characterization techniques. In the case of the PELTOR-OPTIME-98, it is seen in Figs. 4(d) and 4(e) that the FDZ model fitted on case (2) provides higher loss factor values than the FDZ model fitted on case (1): it is equal to 0.8 and 0.6, respectively, at 200 Hz, where the pumping motion occurs. Therefore, it is expected that if the loss factor assessed from case (2) is used, a higher IL will be obtained at the pumping resonance.

V. RESULTS AND DISCUSSION

A. SF model

Figure 5 compares the IL predicted using the SF model with the experimental data for both HPDs. The light gray curves represent the computed ILs calculated with the four frequency-independent equivalent stiffnesses associated to the compression rates measured at points A, B, C, and D. In

TABLE V. FE models and related mechanical parameters of the PELTOR-OPTIME-98 cushion.

Cushion model	ρ (kg/m^3)	ν (1)	α (1)	M_0 (N/m or Pa)	M_∞ (N/m or Pa)	t_r (s)
Spring foundation case (1)	—	—	0.58486	32 941	2 720 079	8.17×10^{-7}
Spring foundation case (2)	—	—	0.5292	20 341	3 525 021	7.2629×10^{-7}
Equivalent solid	84	0.4	0.5838	41 597	3 858 224	6.58×10^{-7}
		0.3	0.58347	53 617	4 810 947	6.97×10^{-7}
		0.0	0.58389	64 834	5 374 537	8.03×10^{-7}

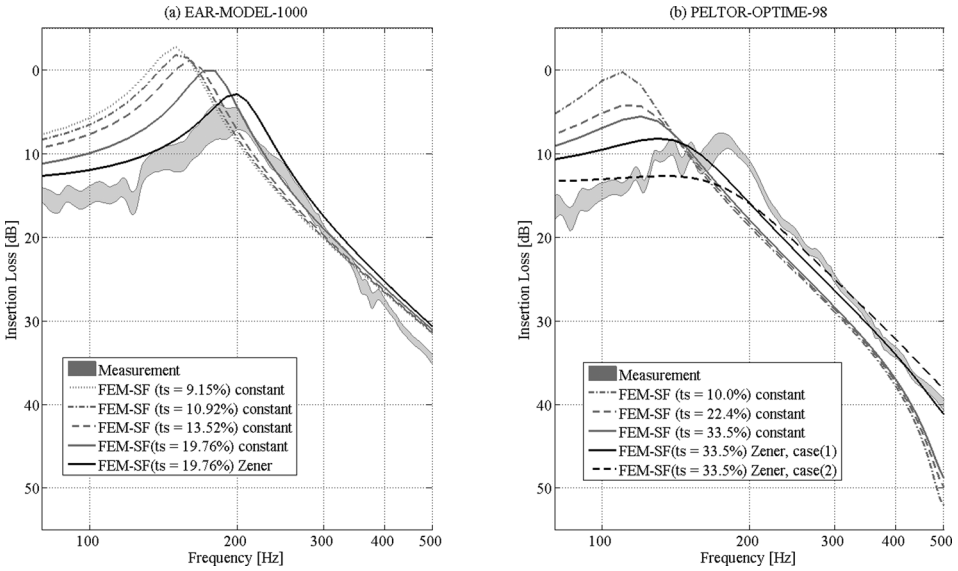

FIG. 5. Earmuff IL measured and predicted with the FEM model using the spring foundation cushion model. Influence of the static compression rate for frequency-independent mechanical parameters and influence of the frequency-dependence of the mechanical parameters at a given static compression rate: (a) EAR-MODEL-1000, (b) PELTOR-OPTIME-98.

the case of the PELTOR-OPTIME-98, the simulation carried out with the equivalent stiffness associated to $\tau_s = 22.4\%$ corresponds to both points A and C (see Table III). The solid black line represents the IL computed with the frequency-dependent mechanical parameters associated to the maximum compression rate [$\tau_s = 19.8\%$ for EAR-MODEL-1000 and $\tau_s = 33.5\%$ for the PELTOR-OPTIME-98, Figs. 4(a), 4(b), 4(d), 4(e)]. The light gray envelope is the confidence interval of IL measurements. As explained in Boyer *et al.* (2014), the measurement uncertainties account for material inhomogeneity (five different samples per earmuff were investigated) and mounting condition effects (three tests were run for each configuration and the sample was taken off and reinstalled between each measurement).

For both earmuffs, a poor correlation between models and experimental data is found below and around the pumping resonance frequency when using frequency-independent mechanical parameters. As expected, the highest cushion compression rate provides the highest equivalent stiffness and the highest IL in this frequency range. However, it is not sufficient to match the measurements. The use of frequency-dependent parameters through the FDZ model leads to a closer approximation of the measured IL. This corroborates the work of Anwar (2005). For the EAR-MODEL-1000, a relatively good agreement is found between model and measurements; the pumping resonance is predicted at the right frequency at 200 Hz. However, a bias in amplitude of $\sim$3 dB can be observed below and around this frequency. This difference might be attributed to the boundary conditions at the interface cushion-baffle which are different in the measurements (acoustic sealant is used to control leaks, see Boyer *et al.* (2014) and the model (cushion is assumed clamped to the baffle).

Similar conclusions can be drawn for the PELTOR-OPTIME-98. However, discrepancies between simulations and measurements are more important for frequencies below the pumping resonance. This can be attributed to an added stiffness brought by the acoustic sealant, which impacts more strongly the PELTOR-OPTIME-98 cushion made of a very flexible sheath. It is seen that using FDZ parameters of case (2) leads to a higher IL than case (1) below and around the pumping motion resonance [compare solid and dashed black curves in Fig. 5(b)]. This is caused by both a higher equivalent stiffness, which makes the IL increase below the pumping motion, and a higher loss factor, which damps the pumping resonance. Thus, after the pumping motion, the IL of case (2) is slightly decreased compared to case (1) because the pumping resonance frequency is translated toward higher frequencies. In the following, FDZ parameters obtained for case (1) are used as they lead to a better representation of the pumping motion.

B. ES model

The ES model which accounts for the 3D cushion deformation is investigated in this section. The focus is put on (1) the effect of the Poisson's ratio used in the inverse characterization procedure (see Sec. IV B) and (2) the influence of the acoustical excitation on the cushion's flanks. Indeed, neglecting the sound excitation of the cushion flanks is *a priori* a reasonable assumption (Boyer *et al.*, 2014) since the sound attenuation of the cushion alone (i.e., when the cup is replaced by a thick and heavy metal plate and when the pumping motion was "disabled") was found to be between 40 and 50 dB for the EAR-MODEL-1000 and between 45 and 55 dB for the PELTOR-OPTIME-98 from 20 Hz to 900 Hz, respectively. The SF model implicitly fulfills this assumption since no sound is allowed to be transmitted through the cushion flanks. On the contrary, sound can be transmitted through the cushion flanks in the ES model. Therefore, in order to compare the results of the SF and ES models, the cushion flanks should not be excited in the ES model. It is, however, interesting to see how the sound path through the cushion flanks affects the response of the earmuff at low frequency when the cushion is coupled to a plastic cup and not a metal plate as in Boyer *et al.* (2014). This justifies the discussion about the effects of the cushion flanks sound excitation. According to Sec. V A, all simulations are now carried out with frequency-dependent parameters associated to the maximum *in situ* static compression rates.

Furthermore, the loss factor of the PELTOR-OPTIME-98 cushion used in the simulations corresponds to case (1).

1. Effect of Poisson's ratio

Figures 6(a) and 6(c) compare the IL predicted with the ES model for three different Poisson's ratios ($\nu = 0$, 0.3, 0.4), the SF model, and the experimental data. In these simulation results, the cushion's flanks are not excited in order to mimic the SF configuration in which no sound is transmitted through the cushion flanks. The case where they are excited is discussed in Sec. V B 2. It is shown that: (1) the ES model provides similar ILs as the SF model, (2) the IL computed for $\nu = 0$ (no bulging effect) is, as expected, identical to the one calculated with the SF model, and (3) the IL slightly decreases as the Poisson's ratio increases. The later Poisson's ratio effect is due to the fact that, for a given cushion equivalent stiffness, the inverse numerical procedure presented in Sec. IV B provides lower equivalent Young's moduli when the Poisson's ratio increases [see Figs. 4(c)–4(f)].

2. Effect of the sound excitation on cushion's flanks

The effect of the sound excitation on the cushion's flanks in the ES model is investigated in Figs. 6(b) and 6(d) for the three different Poisson's ratios. It is seen that, for both HPDs, the computed ILs using the different Poisson's ratios are superimposed with the SF model, up to 350 Hz for the EAR-MODEL-1000 and, on the whole, studied frequency band for the PELTOR-OPTIME-98. When comparing Figs. 6(a) and 6(b) for the EAR-MODEL-1000 and Figs. 6(c) and 6(d) for the PELTOR-OPTIME-98, it is seen that a higher IL is computed when the sound excitation on the cushion's flanks is taken into account (except for $\nu = 0$, for which the IL is not sensitive to cushion acoustic excitation). This was not expected since *a priori* energy can flow through the cushion walls and be transmitted to the inner cavity. Additional computations showed that the sound pressure transmitted through the cushion flanks interferes destructively with that transmitted through the cup, leading therefore to a higher attenuation. This effect is less important in the case of $\nu = 0$ since, in that case, the equivalent Young's modulus is higher [see Figs. 4(c) and 4(f)], the cushion low frequency sound transmission loss thus increases and, consequently, the interference phenomenon decreases.

According to the later results associated to the ES cushion modeling, it is advised to excite the cushion' flanks, since in that case, the low frequency IL is barely sensitive to the chosen Poisson's coefficient. However, this conclusion has to be examined at higher frequencies.

C. LPM model

A LPM is generally used to predict the low frequency response of earmuffs. In this section, the LPM based on either the Du and Homma formulation or the Sides (2004) formulation described in Sec. II is applied to the two commercial earmuffs. These models also require the knowledge of the frequency-dependent complex stiffness characterized in Sec. IV. Figure 7 displays the experimental ILs and the LPM simulations. It has to be recalled that both formulations differ by the definition of the surface, S_r. Furthermore, as

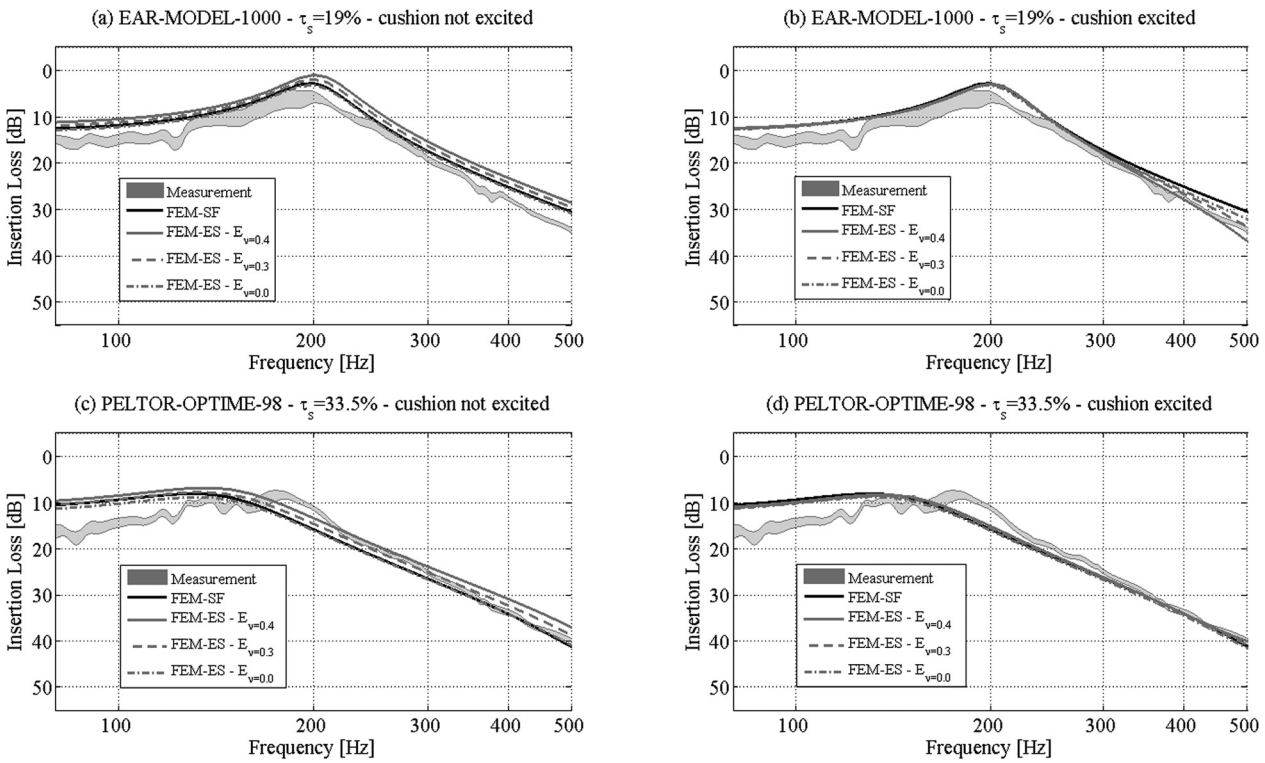

FIG. 6. Earmuff IL measured and predicted with the FEM model using the ES model of the cushion. [First line, (a) and (b)] EAR-MODEL-1000 with $\tau_s = 19.8\%$, [second line, (c) and (d)] PELTOR-OPTIME-98 with $\tau_s = 33.5\%$; (first column) cushion not excited, (second column) cushion excited. The frequency-dependent mechanical parameters are used in all simulations. The Zener model related to case (1) is used in all PELTOR-OPTIME-98 simulations.

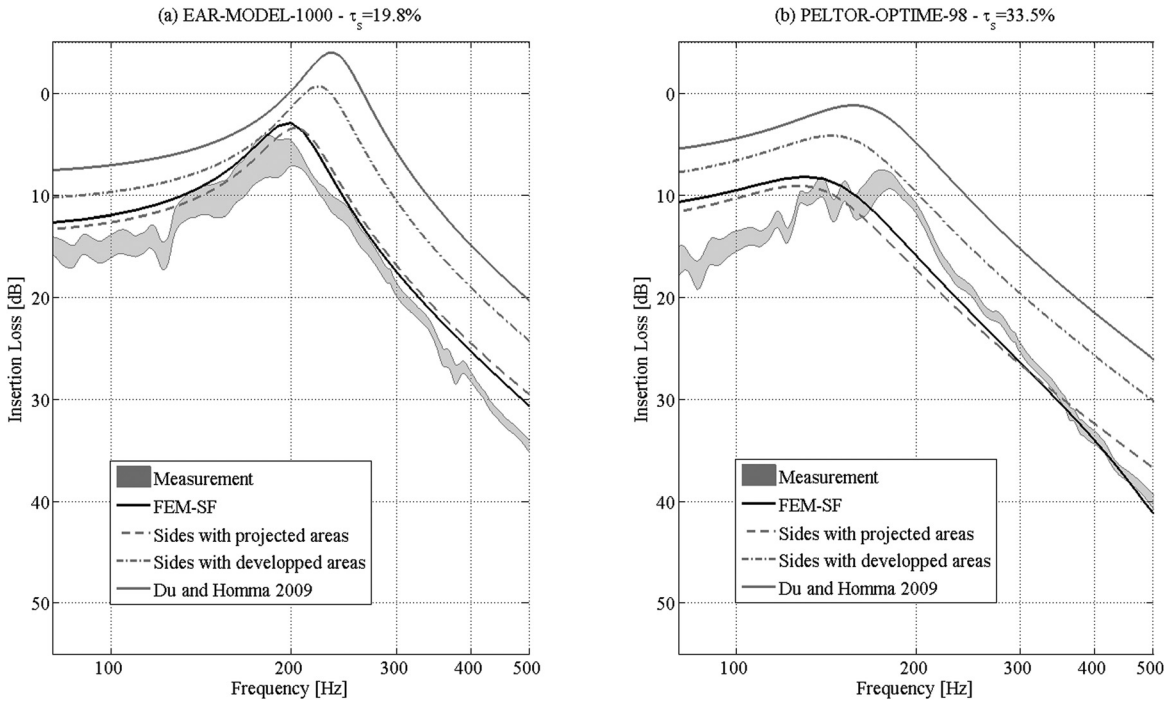

FIG. 7. LPM of the studied commercial earmuff, using the Du and Homma formulation or the Sides formulation; (a) EAR-MODEL-1000 with $\tau_s = 19.8\%$, (b) PELTOR-OPTIME-98 with $\tau_s = 33.5\%$. The frequency-dependent mechanical parameters are used in all simulations. The Zener model related to case (1) is used in all PELTOR-OPTIME-98 simulations.

mentioned in Sec. II, the calculations based on Sides's formulation are carried out twice considering either the developed or projected areas for S_o and S_i. Indeed, the use of developed areas seems *a priori* more consistent with the definition of S_o and S_i.

For the two studied HPDs, Fig. 7 shows that the Sides formulation using the projected areas provides the most accurate IL prediction. This simulated IL is also close to the one calculated with the SF model (on the whole studied frequency band for the EAR-MODEL-1000, and up to 350 Hz for the PELTOR-OPTIME-98). For the other formulations, significant discrepancies are observed as the air cavity stiffness is not well estimated: e.g., the area computed using the Du and Homma's formula, $S_r^{(1)}$, is almost twice the one computed with the Sides (2004) formulation, $S_r^{(2)}$, with the projected area (see Table I). It is important to recall that in this work, the air volume and the various areas have been accurately estimated from the CAD models. However, the 3D numerical geometries are, generally, not available and the aforementioned parameters need to be adjusted to fit the LPM model with the experimental results.

VI. CONCLUSION

This paper was interested in evaluating two FE models and a LPM to predict the sound attenuation of earmuffs in the low frequency range where the earmuff acoustical behavior is governed by the pumping motion. The two FE models consider either the foam-filled cushion as a SF or as an equivalent viscoelastic solid (ES). These models were used to calculate the acoustic response of two commercial earmuffs: the EAR-MODEL-1000 and the PELTOR-OPTIME-98.

A thorough characterization of the equivalent complex stiffness of the foam-filled cushions was proposed. It is based on two complementary low frequency characterization methods (valid for $f < 60$ Hz) associated with a model of the rheological behavior of linear viscoelastic materials in order to estimate the frequency-dependent mechanical properties (stiffness, Young's modulus, and loss factor) in the frequency range of interest (i.e., $80\,\text{Hz} < f < 500\,\text{Hz}$). In the case where the cushion was modeled as an equivalent solid, an inverse hybrid method combining a structural FE model of the quasistatic experimental setup was developed to assess its equivalent Young's modulus for a given Poisson's ratio. Due to the viscoelastic nature of the cushion, the characterization procedure is performed using loading, boundary, and environmental conditions as close as possible to *in situ* conditions. This characterization procedure revealed (i) the important impact of the static compression rate on the measured cushion equivalent mechanical parameters and (ii) the frequency dependence of the equivalent mechanical parameters, which were already observed by Anwar (2005), but not discussed. It was also observed that the equivalent stiffness and loss factor of the two commercial earmuffs behave very differently as a function of frequency and static compression rate. This difference of behavior was attributed to the sheath rigidity (much more important in the case of the EAR-MODEL-1000) and to the presence of an oil pouch in the case of the PELTOR-OPTIME-98. Comparisons between simulations and measurements of the earmuffs attenuation confirm the necessity to account for the frequency dependence of the cushion mechanical parameters. The use of a four-parameter Zener viscoelastic model was found to provide predicted earmuffs attenuations from the

three investigated models (i.e., LPM, SF, and ES) in good agreement with the experimental ones.

Similar attenuation results were obtained with the SF and ES numerical models. However, the use of the SF cushion model should be preferred in this low frequency range since the ES cushion model requires (1) more inputs such as the Poisson's ratio, which is difficult to assess for such complex structure, and (2) a more complex characterization procedure based on an inverse hybrid method coupling FEM calculations and experimental data. However, because it captures 3D elastic deformations, the ES model should provide a more realistic coupling with the back plate, offering a good basis for further computations at higher frequencies. A better agreement between measured and calculated attenuations is also observed when the sound path through the cushion flanks is accounted for using the ES model.

The LPM is straightforward and provides fast results. However, it relies on geometrical parameters with ambiguous definitions, which are difficult to determine precisely if a 3D numerical representation of the structure geometry is not available. Nevertheless, a good prediction was obtained using the Sides formulation, while for the others, large discrepancies with experimental data were observed, caused by a wrong evaluation of the air cavity stiffness.

Future work involves using the FEM model to predict the vibroacoustic behavior of earmuffs at higher frequencies. In particular, the use of the two approaches to model the cushion presented in this paper needs to be discussed at higher frequencies. This will be presented in a forthcoming research paper.

ACKNOWLEDGMENTS

The authors would like to thank IRSST for providing financial support and 3 M for supplying materials, providing the CAD of the PELTOR-OPTIME-98 model and the material properties.

Anwar, A. (**2005**). "Low frequency finite element modeling of passive noise attenuation in ear defenders," Masters thesis, Virginia Polytechnic Institute and State University, Blacksburg, VA, pp. 1–123.

Berger, E. H., Kieper, R. W., and Stergar, M. E. (**2012**). "Performance of new acoustical test fixtures complying with ANSI S1242-2010, with particular attention to the specification of self insertion loss," in *Proceedings of Internoise 2012*, New York, New York, pp. 517–528.

Boyer, S., Doutres, O., Sgard, F., Laville, F., and Boutin, J. (**2013**). "Sound transfer path analysis to model the vibroacoustic behaviour of a commercial earmuff," in *Proceedings of Meetings on Acoustics (ICA) 2013*, Montreal, Vol. 19, pp. 1–9.

Boyer, S., Doutres, O., Sgard, F., Laville, F., and Boutin, J. (**2014**). "Objective assessment of the sound paths through earmuff components," Appl. Acoust. **83**, 76–85.

Boyer, S., Sgard, F., and Laville, F. (**2011**). "Development of an equivalent solid model to predict the vibroacoustic behaviour of earmuff cushions," in *Proceedings of the Meeting Acoustics Week in Canada*, Québec City, Vol. 39, No. 3, pp. 96–97.

Du, Y., and Homma, K. (**2009**). "Performance of a dual-cup-dual cushion earmuff design," Noise Control Eng. J. **57**, 459–475.

Gerges, S. N. (**2012**). "Earmuff comfort," Appl. Acoust. **73**, 1003–1012.

James, C. (**2006**). "Finite element modeling and exploration of double hearing protection systems," Masters thesis, Virginia Polytechnic Institute and State University, Blacksburg, VA, pp. 1–147.

Kalb, J. T. (**2010**). "A hearing protector model for predicting impulsive noise hazard," J. Acoust. Soc. Am. **127**, 1879.

Khani, M., Riyad, K., and Azzeddine, S. (**2007**). "Finite element analysis of an earmuff-earcanal system," Can. Acoust. **35**, 66–67.

Langlois, C., Panneton, R., and Atalla, N. (**2001**). "Polynomial relations for quasi-static mechanical characterization of isotropic poroelastic materials," J. Acoust. Soc. Am. **110**, 3032–3040.

Lee, C.-M., Royster, L. H., and Ciskowski, R. D. (**1995**). "Formulation for an FE and BE coupled problem and its application to the earmuff-earcanal system," Eng. Anal. Bound. Elem. **16**, 305–315.

Paakkonen, R. (**1992**). "Effects of cup, cushion, band force, foam lining and various design parameters on the attenuation of earmuffs," Noise Control Eng. J. **38**, 59–65.

Paurobally, M. R., and Pan, J. (**2000**). "The mechanisms of passive ear defenders," Appl. Acoust. **60**, 293–311.

Pritz, T. (**1996**). "Analysis of four-parameter fractional derivative model of real solid materials," J. Sound Vib. **195**, 103–115.

Rodriguez, E. E., and Gesnouin, G. A. (**2007**). "Effective mass of an oscillating spring," Phys. Teach. **45**, 100–103.

Sahraoui, S., Mariez, E., and Etchessahar, M. (**2000**). "Mechanical testing of polymeric foams at low frequency," Polym. Test. **20**, 93–96.

Sgard, F., Nélisse, H., Gaudreau, M.-A., Boutin, J., Voix, J., and Laville, F. (**2010**). "Study of sound transmission through hearing protection device and application of a method to better assess their real efficiency in workplace. Part 2: Preliminary study of finite element models of hearing protection devices," Technical Report No. 099-494 (IRSST, Montreal), pp. 1–106 (in French).

Shaw, E. A. G. (**1979**). "Hearing protector attenuation: A perspective view," Appl. Acoust. **12**, 139–157.

Shaw, E. A. G., and Thiessen, G. J. (**1958**). "Improved cushion for ear defender," J. Acoust. Soc. Am. **30**, 24–36.

Shaw, E. A. G., and Thiessen, G. J. (**1962**). "Acoustics of circumaural earphones," J. Acoust. Soc. Am. **34**, 1233–1246.

Sides, J. D. (**2004**). "Low frequency modeling and experimental validation of passive noise attenuation in ear defenders," Masters thesis, Virginia Polytechnic Institute and State University, Blacksburg, VA, pp. 1–96.

Vergara, F., Gerges, S. N., and Birch, R. S. (**2002**). "Numerical and experimental study of impulsive sound attenuation of an earmuff," Shock Vib. **9**, 245–251.

Zwislocki, J. (**1955**). "Factors determining the sound attenuation produced by earphone sockets," J. Acoust. Soc. Am. **27**, 146–154.